Torus Instability as trigger mechanism for CMEs: the 2011 August 4 filament eruption

F. P. Zuccarello, D. B. Seaton, M. Mierla, S. Poedts, L. A. Rachmeler, P. Romano, and F. Zuccarello

Introduction

We present an analysis of the observation of a filament eruption that agrees with the torus instability model. This model predicts that a magnetic flux rope embedded in an ambient field undergoes an eruption when the axis of the flux rope reaches a critical height that depends on the topology of the ambient field. We use the two vantage points of SDO and STEREO to reconstruct the three-dimensional shape of the filament, to follow its morphological evolution and to determine its height just before the eruption. The magnetograms acquired by SDO/HMI are used to infer the topology of the ambient field and to derive the critical height for the onset of the torus instability.

1. Active region evolution

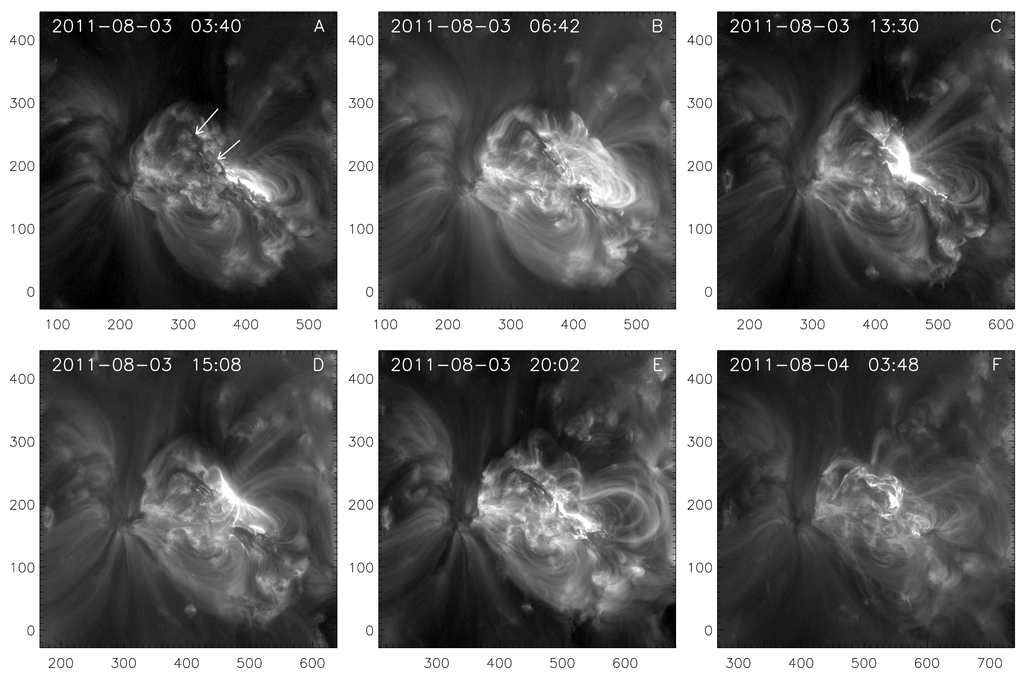

Fig. 1. Sequence of co-aligned AIA 193 Å images. The white arrows indicate two filaments. **On August 3 at 13:17 UT an M6.0 flare occurred close to the foot point of the northern filament, without destabilizing it.** On August 4 at 03:48 the filament erupted completely.

2. Morphology

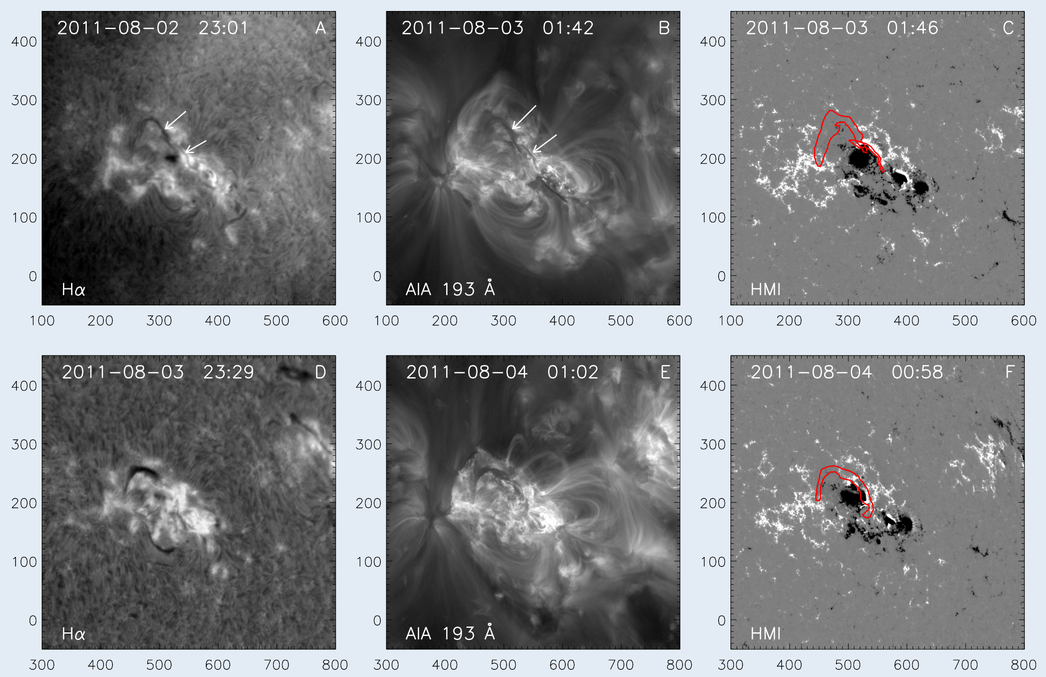

Fig. 2. Co-aligned images of the active region taken before (top) and after (bottom) the M6.0 flare that occurred on August 3 at 13:17 UT. The red contours on the magnetograms outline the shape of the analyzed filaments. **The magnetic configuration suggests that the two filaments are part of the same complex flux rope.**

3. Three-dimensional reconstruction

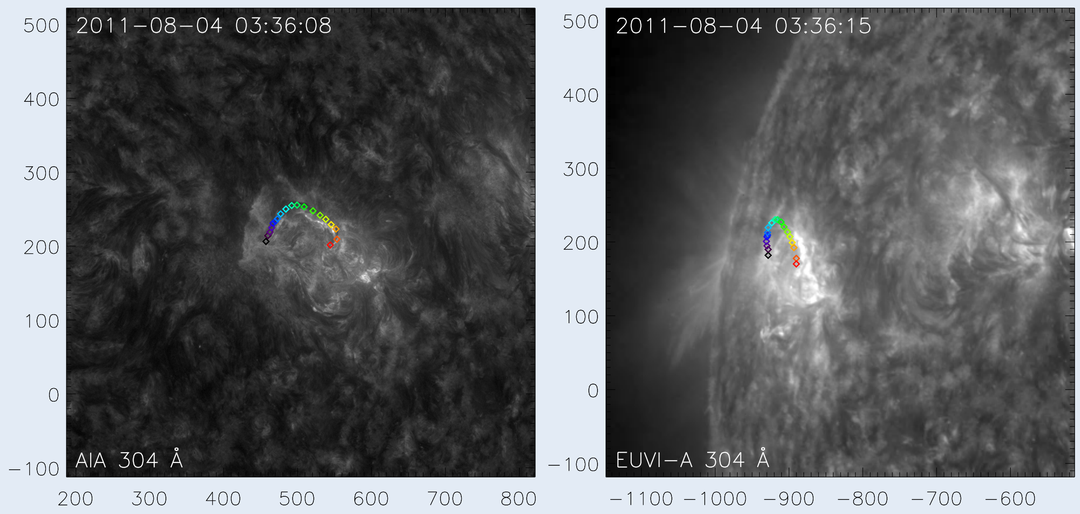

Fig. 3. 3D reconstruction of the filament (cross-referenced colored diamonds) projected on AIA and EUVI-A images. **We performed three reconstructions: first, on August 3 at 08:35, before the M6.0 flare; second, on August 3 at 21:36, about six hours after the M6.0 flare; and, third, on August 4 at 03:36, just before the filament eruption.**

4. Decay index & torus instability

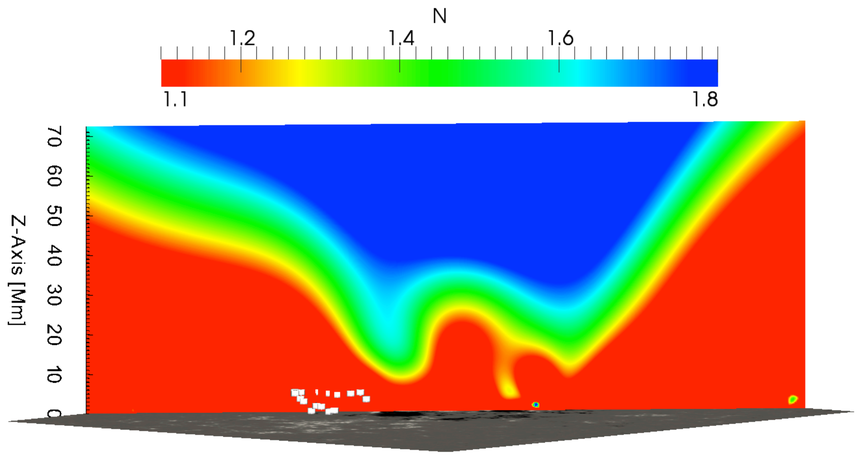

Fig. 4. Plot of the decay index along a plane passing through the axis of the filament (white cubes) for the potential field extrapolation on August 3 at 06:00 UT. The torus instability threshold is indicated in yellow-green (n_{crit}=1.3-1.5). **When the M6.0 flare occurred the filament was stable with respect to torus instability.**

Fig. 5. Plot of the decay index for the potential field extrapolation on August 4 at 03:36 UT. The white and black cubes highlight the 3D position of the filament on August 3 at 21:36 UT and on August 4 at 03:36 UT. **After the M6.0 flare, the filament approaches an unstable region.**

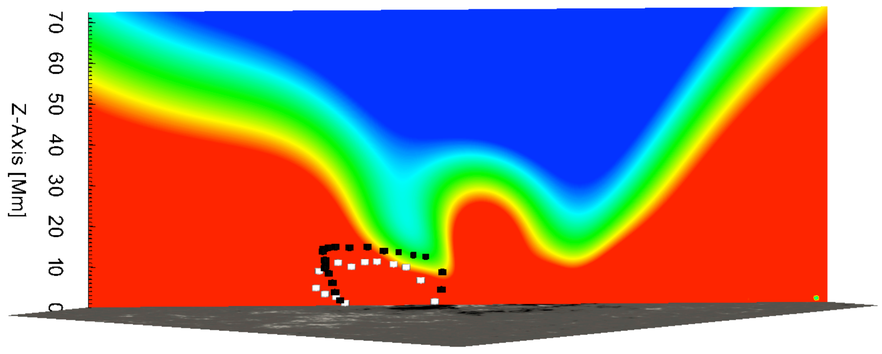

5. Flux cancellation

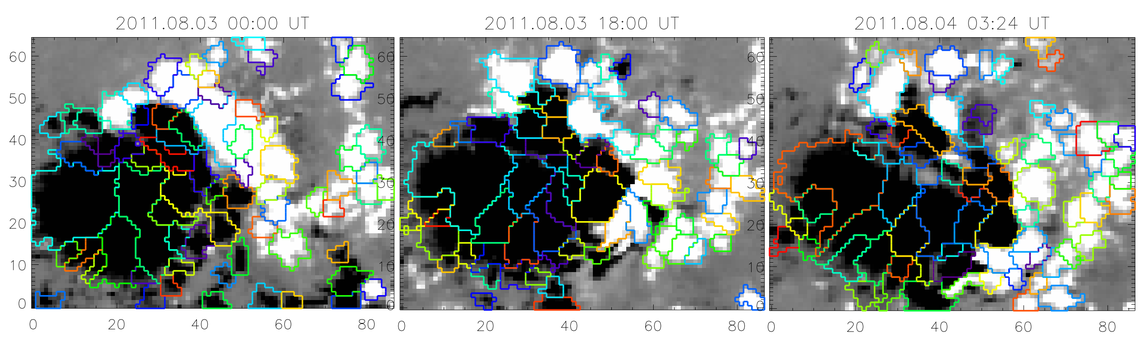

Fig. 6. Top: Zoom of the HMI magnetograms. The color contours highlight different magnetic features identified using the YAFTA algorithm. Right: Time evolution of the positive (dash-dotted red), negative (dashed black) and total unsigned (solid blue) magnetic flux for the region shown in the top panels.

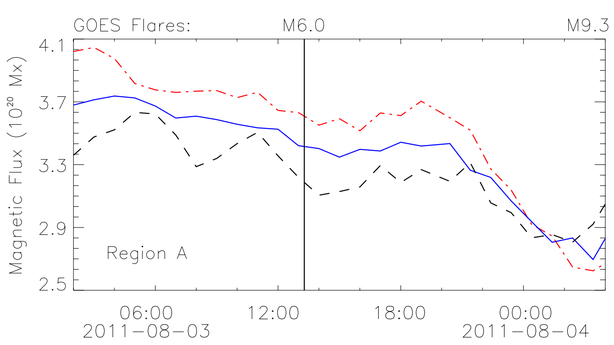

Conclusion

Combining three-dimensional reconstructions of the filament and potential magnetic field extrapolations, we show that the trigger of the eruption was the torus instability. Our analysis also shows that the change in the morphology of the filament and the observed flux cancellation were fundamental to facilitating the eruption. In fact, due to the change in its morphology, the pre-eruption filament extended south into a region where the magnetic field was more vulnerable. In this new configuration, the flux cancellation removed part of the line-tying, allowing the rise of the filament up to the height where the decay index is larger than n_{crit}=1.3-1.5, eventually resulting in an eruption.